Supersymmetric dark matter in light of WMAP

T. Nihei (Nihon Univ.)

July. 30, 2003 at KEK

References

[1] Ellis–Olive–Santoso–Spanos, Phys. Lett. B365 (2003) 176.

[2] Kim–T.N–Roszkowski–Ruiz de Austri, JHEP0212 (2002).
T.N.–Roszkowski–Ruiz de Austri, JHEP0207 (2002);
JHEP0203 (2002); JHEP0105 (2001).
Roszkowski–Ruiz de Austri–T.N., JHEP 0108 (2001).

Cosmological observations

Relic density

New CMB observations (Boomerang, MAXIMA, $\cdots$)

$\hookrightarrow 0.1 < \Omega_\chi h^2 < 0.3$

WMAP (2001–, NASA)

$\Omega_m h^2 = 0.135^{+0.008}_{-0.009}$, $\Omega_b h^2 = 0.0224 \pm 0.0009$

$\Omega_\nu h^2 < 0.0067$

$\Omega_i \equiv \rho_i/\rho_c$

$h \approx 0.7$

$H_0 = 100h$ km/s/Mpc

$\longrightarrow$ Relic density of cold dark matter

$$\Omega_\chi h^2 = 0.1126^{+0.016}_{-0.018} \quad (\chi\text{: CDM})$$

WMAP, Planck (2007–) — $\Omega_\chi h^2$ with $\lesssim$ 10 % accuracy

Direct detection

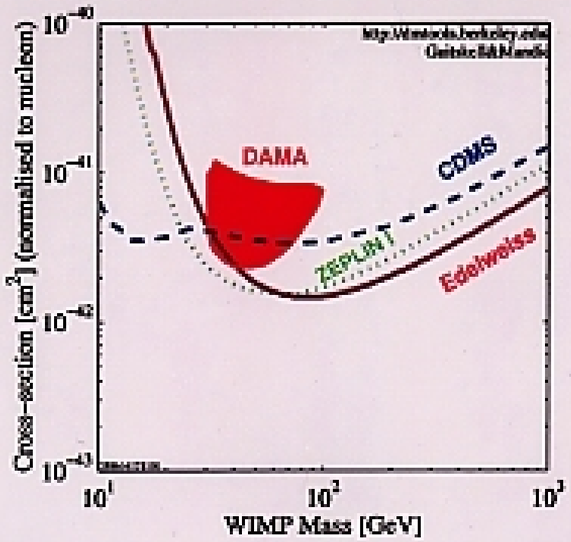

Weakly Interacting Massive Particle (WIMP)

$\chi P \longrightarrow \chi P$

DAMA
CDMS
ZEPLIN
Edelweiss
⋮

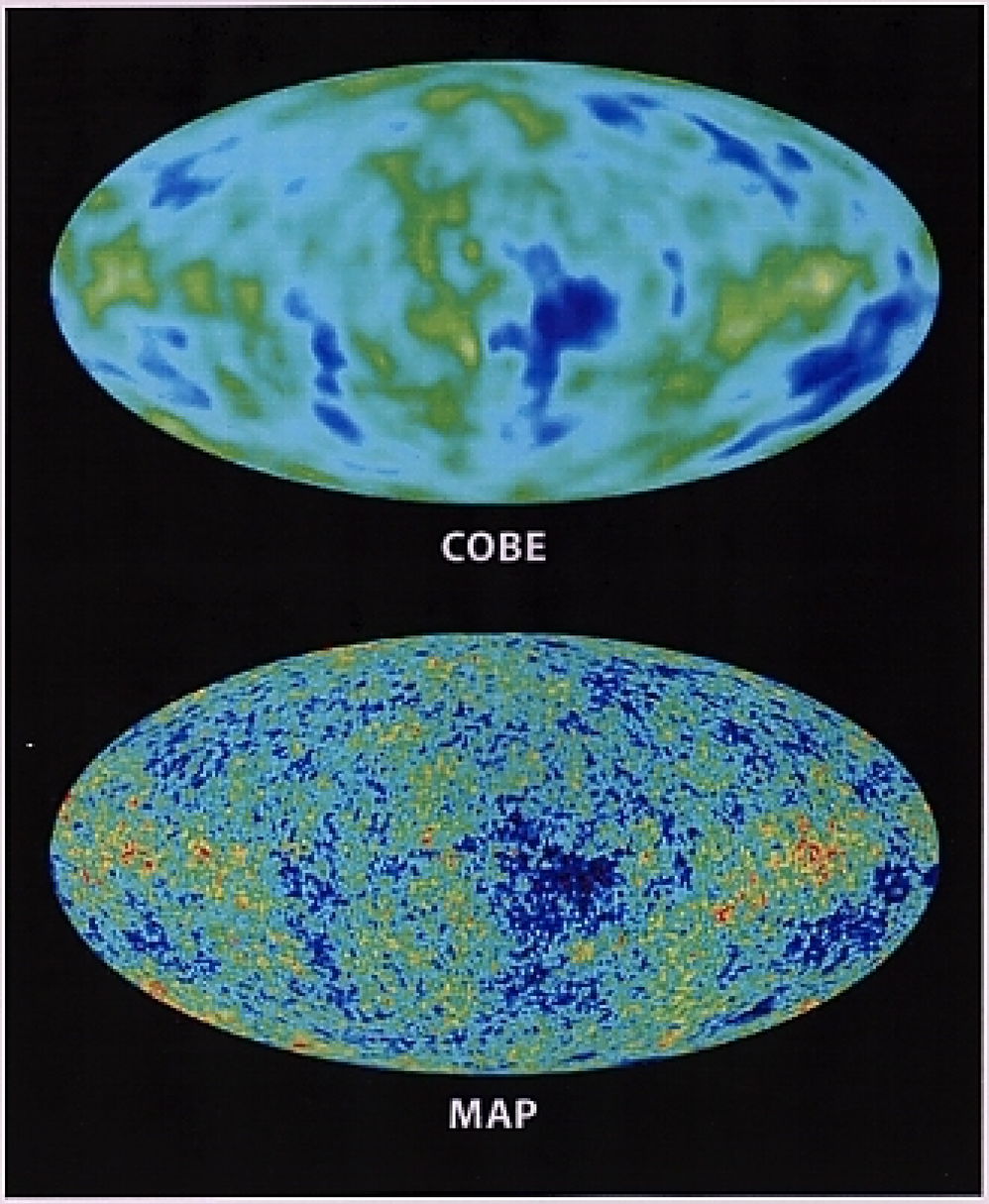

Supersymmetry (SUSY)

Λ: cutoff

- Naturalness

$$m^2_{\rm Higgs} = m_0^2 + \quad + \quad$$
$$= m_0^2 + \alpha\Lambda^2 - \alpha\Lambda^2$$

Quadratic divergence cancelled

superpartners: not discovered yet

$\longrightarrow$ soft SUSY breaking ($\widetilde{m}$)

$$\begin{cases} \text{superpartner: heavy} \\ \Lambda^2 \text{ cancellation: kept} \end{cases}$$

$\longrightarrow$ $\widetilde{m} = 100$ GeV – a few TeV

$$m^2_{\rm Higgs} = m_0^2 + \alpha\widetilde{m}^2$$

- Gauge coupling unification

Non SUSY

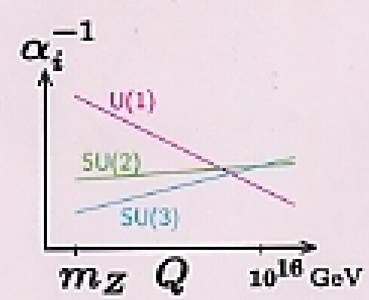

SUSY

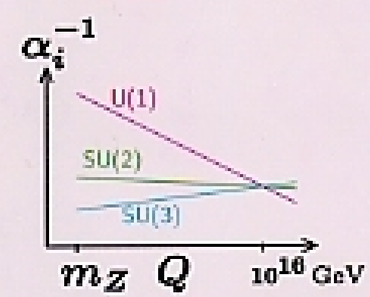

Minimal supersymmetric SM (MSSM)

- Particle contents:

spin = 0	1/2	1
$\tilde{q}\ \tilde{u}\ \tilde{d}$	$q\ u\ d$	
$\tilde{\ell}\ \tilde{e}$	$\ell\ e$	
$H_1\ H_2$	$\widetilde{H}_1\ \widetilde{H}_2$	
	$\widetilde{B}\ \widetilde{W}^a\ \tilde{g}^a$	$B_\mu\ W^a_\mu\ g^\alpha_\mu$

Higgses $h^0, H^0, A^0, H^\pm$

-ino mass eigenstates

$$\begin{cases} \widetilde{H}_1^-, \widetilde{H}_2^+, \widetilde{W}^1, \widetilde{W}^2 \longrightarrow \text{charginos} \quad \chi^\pm_{1,2} \\ \widetilde{H}_1^0, \widetilde{H}_2^0, \widetilde{B}, \widetilde{W}^3 \longrightarrow \text{neutralinos} \quad \chi^0_{1,2,3,4} \end{cases}$$

Majorana

R-parity $\longrightarrow$ Lightest Super Particle (LSP): stable

$\longrightarrow$ DM candidate ($\chi = \chi^0_1$)

- Relevant terms:

gaugino mass $\quad \frac{1}{2}(M_1\widetilde{B}\widetilde{B} + M_2\widetilde{W}^a\widetilde{W}^a + M_3\tilde{g}^a\tilde{g}^a)$

Higgisno mass $\quad \mu\widetilde{H}_1\widetilde{H}_2 + \text{h.c.}$

Higgs mass $\quad \mu^2(|H_1|^2 + |H_2|^2) + \cdots$

$\longrightarrow \tan\beta = \langle H_2^0\rangle/\langle H_1^0\rangle,\ m_A^2|A|^2$

sfermion mass $\quad m^2_{\tilde{q}_i}|\tilde{q}_i|^2 + m^2_{\tilde{\ell}_i}|\tilde{\ell}_i|^2 + \cdots$

(+ scalar trilinear couplings $A_t\tilde{t}_R^\dagger\tilde{q}_L H_2 + \cdots$)

[cf. Constrained MSSM (CMSSM)
$m_0,\ m_{1/2},\ A_0,\ \tan\beta,\ \text{sgn}(\mu)$]

R-parity

$$R = \begin{cases} +1 & \text{SM particles} \\ -1 & \text{superpartners} \end{cases}$$

Without R-parity,

Rapid proton decay via dim4 op.

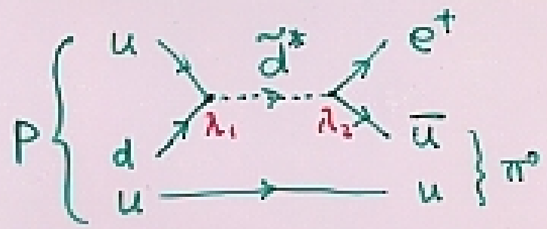

λ_1, λ_2 (dim = 0) $\rightarrow$ unnatually small

R-parity $\rightarrow$ LSP is stable

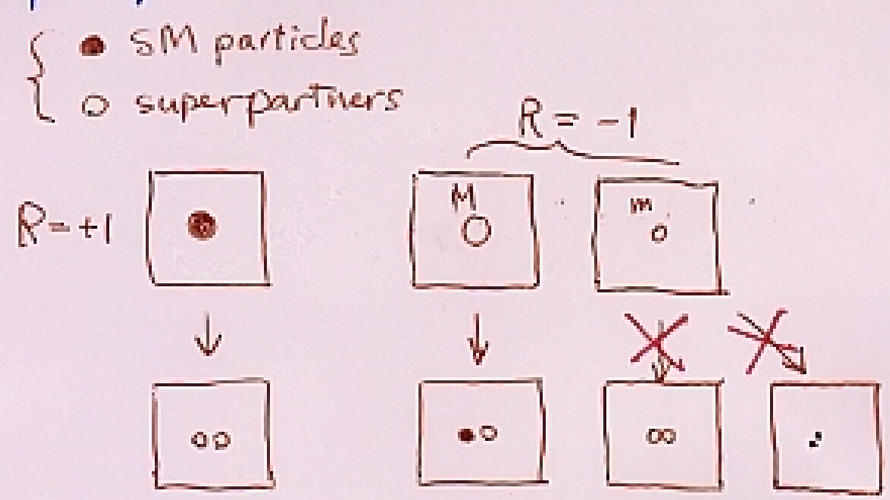

Constrained MSSM (CMSSM)

- Soft SUSY parameters at $Q = M_{\rm GUT}$ ($\approx 2 \times 10^{16}$ GeV)

scalars	$m^2_{\tilde q_i} = m^2_{\tilde \ell_i} = m^2_{H_1} = m^2_{H_2} = m_0^2$
gauginos	$M_1 = M_2 = M_3 = m_{1/2}$
trilinear	$A_{U,D,E} = A_0 Y_{U,D,E}$

- RGE: $M_{\rm GUT} \longrightarrow m_Z$

@ $Q = m_Z$
$M_1 \approx M_2/2$
$M_3 \approx 3M_2$

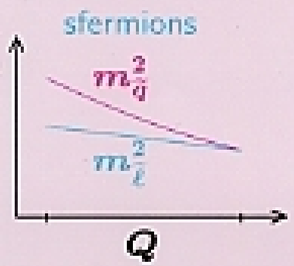

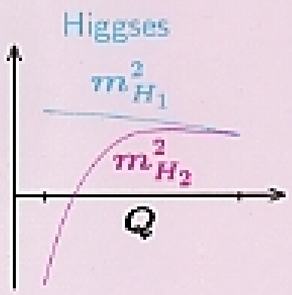

Radiative EW symmetry breaking (EWSB)

$m^2_{\rm Higgs} = m_0^2 > 0$ at $M_{\rm GUT}$

$\longrightarrow m^2_{\rm Higgs} < 0$ at m_Z

$$\left[\frac{m_Z^2}{2} = \frac{m^2_{H_1} - m^2_{H_2}\tan^2\beta}{\tan^2\beta - 1} - \mu^2\right]$$

$\Downarrow$

$4 + 1$ parameters

$m_0,\ m_{1/2},\ A_0,\ \tan\beta,\ {\rm sgn}(\mu)$

Experimental constraints

LEP

- Chargino mass bound: $m_{\chi_1^\pm} > 104\,{\rm GeV}$
- Lightest Higgs mass bound: $m_h > 114\,{\rm GeV}$ (SM)

  $\longrightarrow$ conservative bound: $m_h > 111\,{\rm GeV}$ $\quad m_A$ dep.

$b \to s\gamma$

CLEO, BELLE

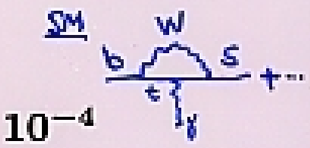

$${\rm Br}(B \to X_s\gamma)_{\rm EXP} = (3.41 \pm 0.36) \times 10^{-4}$$

SM prediction: consistent with exp.

$\longrightarrow$ conservative bound

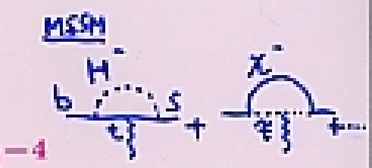

$${\rm Br}(B \to X_s\gamma) = (3.41 \pm 0.67) \times 10^{-4}$$

Dominant NLO SUSY contrib. included

Degrassi–Gambino–Giudice (2000)

Muon $g-2$

E821 experiment (e^+e^- annihilation data) $\qquad a_\mu \equiv (g_\mu - 2)/2$

$$a_\mu^{\rm exp} - a_\mu^{\rm SM} = (33.9 \pm 11.2) \times 10^{-10}$$

3 σ discrepancy

$$11.5 \times 10^{-10} < a_\mu^{\rm SUSY} < 56.3 \times 10^{-10}\ (2\sigma)$$

$$\left[\ 22.7 \times 10^{-10} < a_\mu^{\rm SUSY} < 45.1 \times 10^{-10}\ (1\sigma)\ \right]$$

preferred region

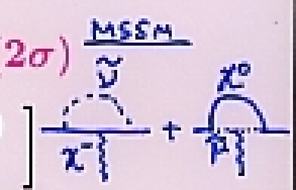

Calculation of relic density

Boltzmann eq.

$$\frac{dn_\chi}{dt} + 3Hn_\chi = -\langle \sigma v_{\rm rel}\rangle (n_\chi^2 - n_\chi^{\rm eq2})$$

Accurate calculation

1. All the contributions to $\sigma = \sigma(\chi\chi \to \text{all})$ NRR (2001)

   "all" = $f\bar{f}$, W^+W^-, ZZ, hh, hH, HH, HA, AA, H^+H^-, Zh, ZH, ZA, $W^\pm H^\mp$

2. Exact formula for $\langle \sigma v\rangle$ Gondolo–Gemini (1991)

   $\longleftrightarrow$ expansion $\langle \sigma v\rangle = a + bx$, $x = T/m_\chi$

3. Accurate treatment of Boltzmann eq.

   $\longleftrightarrow$ approximate solution $\tilde{m}\nearrow$, $\Omega h^2 \nearrow$

   $$\rho_\chi \propto 1/\int_0^{x_f} dx \langle \sigma v\rangle, \quad x_f = T_f/m_\chi \sim 1/20$$

4. Coannihilation ($\chi\chi' \to \cdots$, $\chi'\chi' \to \cdots$, $\cdots$) Griest–Seckel (1991)

   Mizuta–Yamaguchi (1993)

   χ': NLSP ($\tilde{\tau}_1$, χ_2^0, $\chi^\pm$, $\cdots$)

   important for $m_{\chi'} \lesssim 1.1 m_\chi$

   $\sigma \to \sigma_{\rm eff}$ enhanced

In our code, $\Omega_\chi h^2$ can be computed reliably.

- $\tilde{h}$–like LSP
- resonance
- coannihilation

$\Big\} \longrightarrow$ small $\Omega_\chi h^2$

$m_A \approx 2m_\chi$

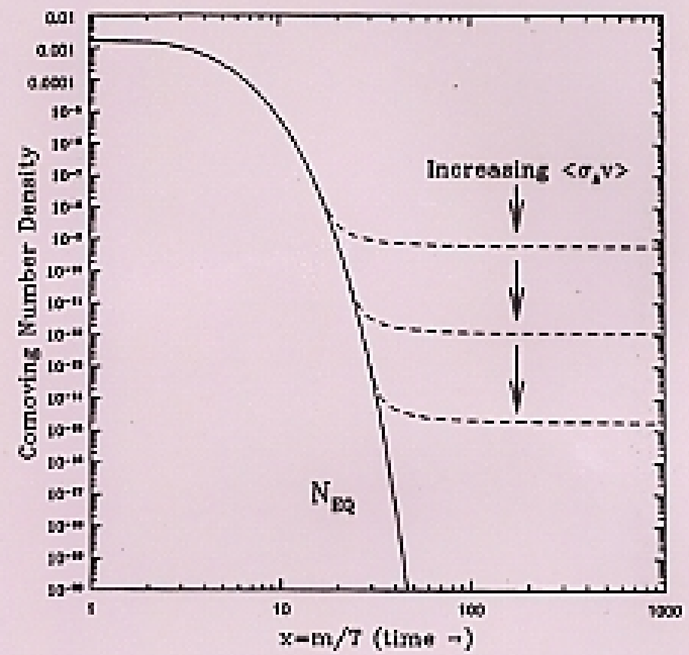

Fig. 4. Comoving number density of a WIMP in the early Universe. The dashed curves are the actual abundance, and the solid curve is the equilibrium abundance. From [31].

interaction rate $\Gamma \sim n\sigma v$

expansion rate $H \sim T^2/M_{Pl}$ (RD)

$\Gamma > H$ thermal

$n_{eq} \sim (mT)^{3/2} e^{-m/T}$ $(T \ll m)$

$\downarrow$

$T_f \approx m_\chi/20$

$\Gamma < H$ decoupled (freeze out)

Cross section $\sigma(\chi\chi \to \text{all})$

Process	s-channel	t & u-channel
$\chi\chi \to f\bar{f}$	h, H, A, Z	$\tilde{f}_{1-6}$
$\chi\chi \to hh, hH, HH$	h, H	χ^0_{1-4}
hA, HA	A, Z	χ^0_{1-4}
AA	h, H	χ^0_{1-4}
H^+H^-	h, H, Z	$\chi^\pm_{1,2}$
$\chi\chi \to W^+W^-$	h, H, Z	$\chi^\pm_{1,2}$
ZZ	h, H	χ^0_{1-4}
$\chi\chi \to Zh, ZH$	A, Z	χ^0_{1-4}
ZA	h, H	χ^0_{1-4}
$W^\pm H^\mp$	h, H, A	$\chi^\pm_{1,2}$

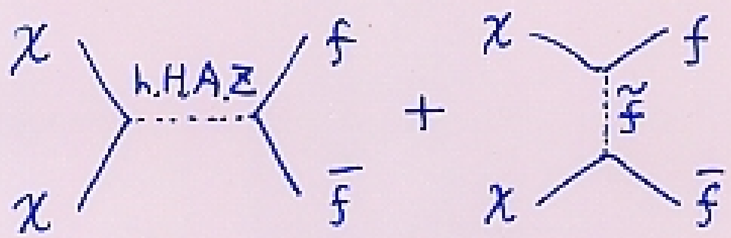

Resonance (pole) at $2m_\chi \simeq m_A$...

$M_1 \ll \mu \longrightarrow \chi \sim \tilde{B} \longrightarrow \sigma$ small

$M_1 \gg \mu \longrightarrow \chi \sim \tilde{H} \longrightarrow \sigma$ large

T.N.-Roszkowski-Ruiz
(JHEP 0105)

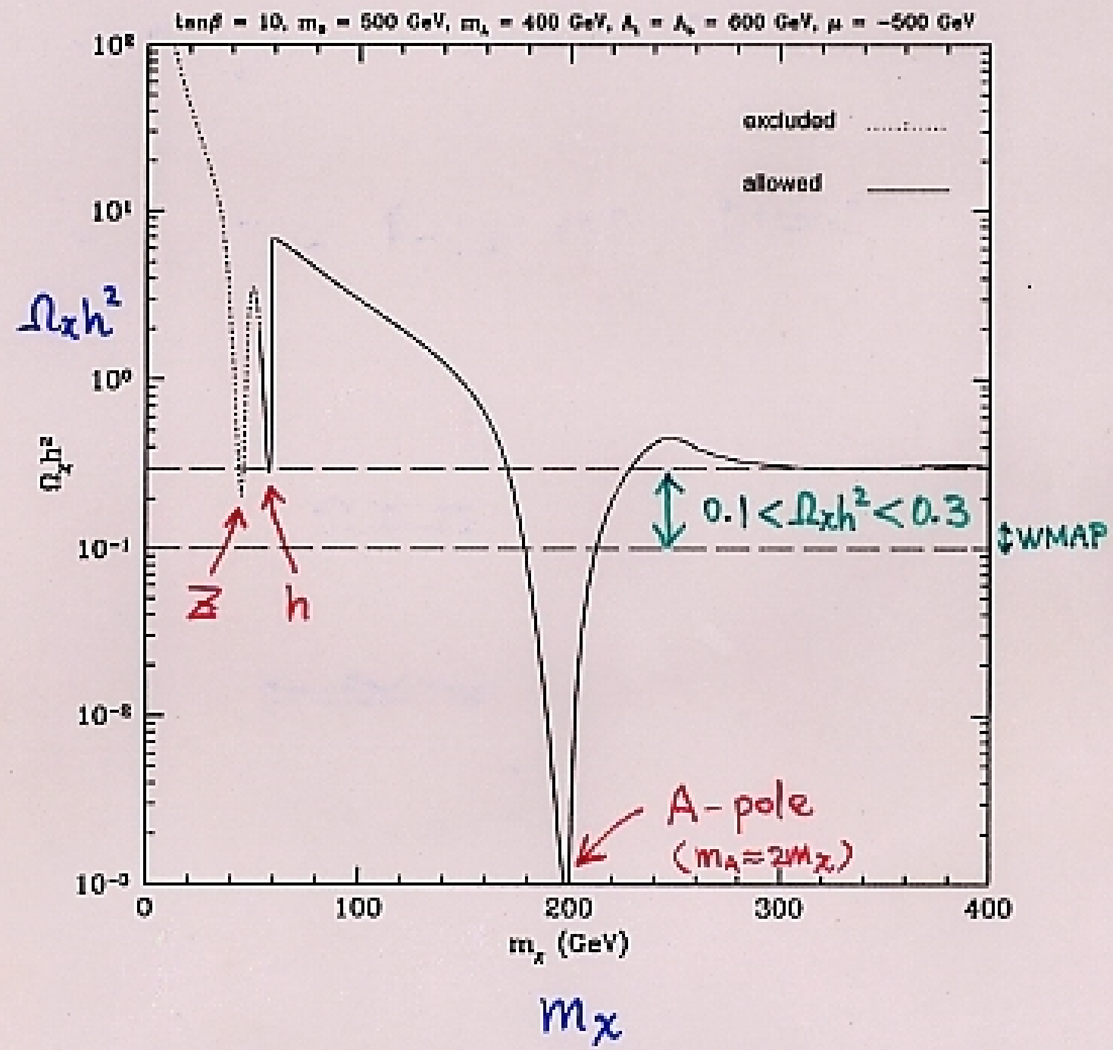

Figure 5: The relic density $\Omega_\chi h^2$ for the same choice of parameters as in figure 1. The solid (dotted) curves are allowed (excluded) by current experimental constraints. Here $\Omega_\chi h^2$ is computed using the exact expressions for the cross section. The band between the two horizontal dashed lines corresponds to the cosmologically favoured range $0.1 < \Omega_\chi h^2 < 0.3$.

Coannihilation

Griest–Seckel (1991)

If NLSP (χ') is nearly degenerate with LSP ($m_{\chi'} \lesssim 1.1 m_\chi$), then

f, f': SM particles

$\chi f \leftrightarrow \chi' f'$ is much faster than $\chi\chi \leftrightarrow f f'$.

$\uparrow$ $\qquad\qquad\qquad\qquad$ $\uparrow$

Reaction rate

$$r_{\chi f} \sim n_\chi n_f \sigma_{\chi f} \sim \sigma_{\chi f} \exp\left(-\frac{m_\chi}{T}\right) \quad \ggg \quad r_{\chi\chi} \sim n_\chi n_\chi \sigma_{\chi\chi} \sim \sigma_{\chi\chi} \exp\left(-\frac{2m_\chi}{T}\right)$$

$$\longrightarrow \left.\begin{array}{l} \sigma(\chi\chi' \to f f') \\ \sigma(\chi'\chi' \to f f') \end{array}\right\} \text{should be included.}$$

can be $\gg \sigma(\chi\chi \to f f')$

- Boltzmann eq. with coannihilation

Replacements

$$\begin{cases} n_\chi & \longrightarrow \quad n = \sum_i n_i \\ \langle \sigma v \rangle & \longrightarrow \quad \langle \sigma_{\rm eff}\, v \rangle = \sum_{i,j} \langle \sigma_{ij} v_{ij} \rangle \frac{n_i^{\rm eq}}{n^{\rm eq}} \frac{n_j^{\rm eq}}{n^{\rm eq}} \end{cases}$$

$\downarrow$

$$\frac{dn}{dt} = -3Hn - \langle \sigma_{\rm eff}\, v \rangle (n^2 - n_{\rm eq}^2)$$

$\sigma \longrightarrow \sigma_{\rm eff}$: enhanced by coann.

- CMSSM: $\chi' = \tilde{\tau}_1$ (common situation)

T.N.-Roszkowski-Ruiz (2002)

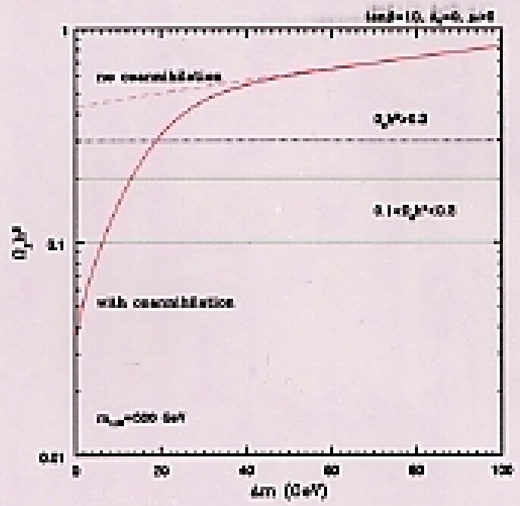

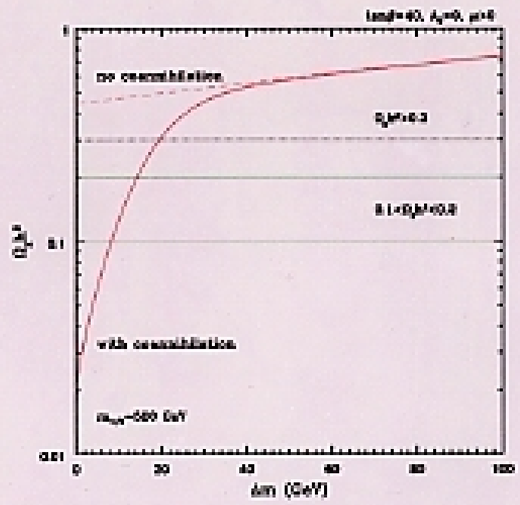

$$\Delta m = m_{\tilde{\tau}_1} - m_\chi$$

Coannihilation

NRR (2002)

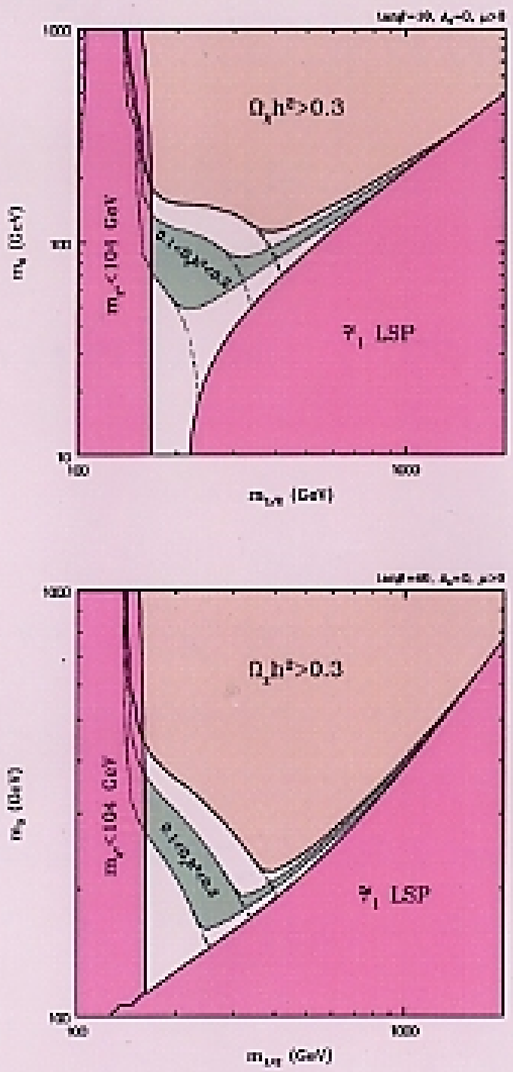

Figure 6: Contours of $\Omega_\chi h^2$ in the plane $(m_{1/2}, m_0)$ for $\tan\beta = 10$ (upper window) and $\tan\beta = 40$ (lower window), and for $A_0 = 0$, $\mu > 0$, $m_t^{pole} = 175$ GeV and $m_b(m_b)^{\overline{MS}}_{SM} = 4.20$ GeV. The red regions bands are excluded by chargino searches at LEP and corresponds to the lighter stau being the LSP. The light orange regions of $\Omega_\chi h^2 > 0.3$ are excluded by cosmology while the narrow green bands correspond to the expected range $0.1 < \Omega_\chi h^2 < 0.2$. Also shown are the semi-oval contours of $\Omega_\chi h^2$ in the absence of coannihilation.

CMSSM

$\tilde{m}\nearrow$, $\Omega h^2 \nearrow$

Roszkowski - Ruiz - T.N.
(JHEP0108)

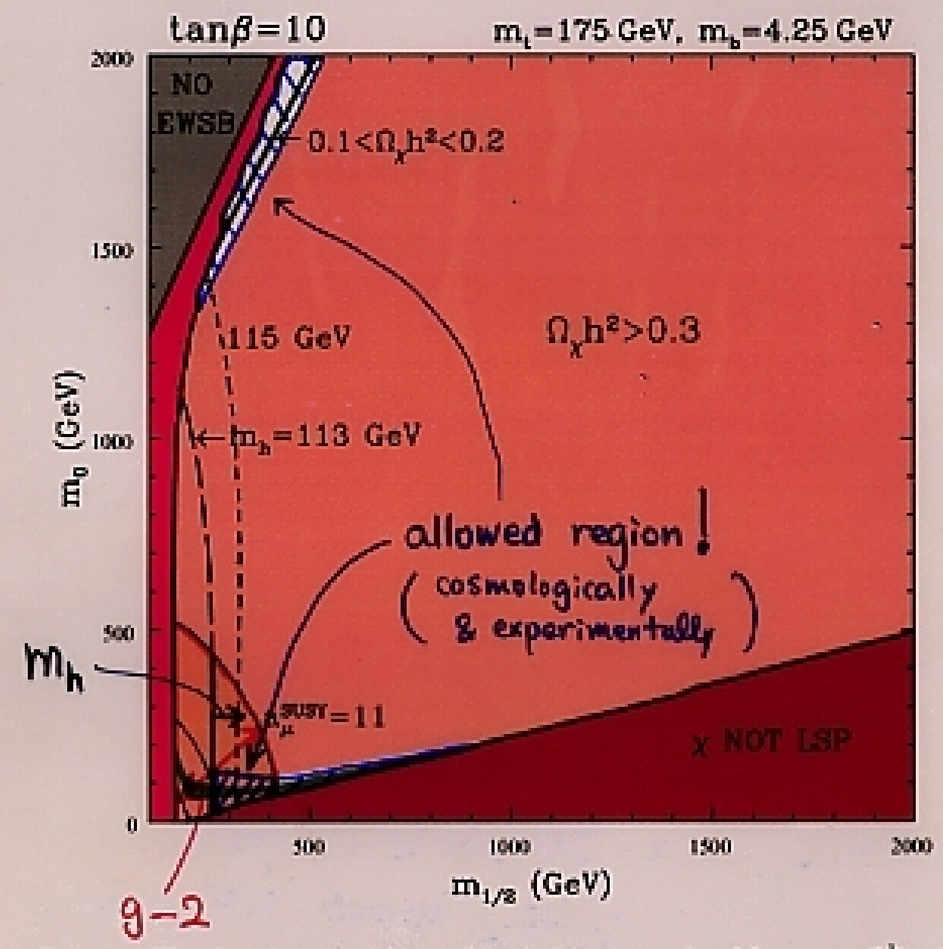

Figure 1: The plane $(m_{1/2}, m_0)$ for $\tan\beta = 10$, $A_0 = 0$, $\mu > 0$ and for $m_t \equiv m_t^{pole} = 175$ GeV and $m_b \equiv m_b(m_b)^{\overline{MS}}_{SM} = 4.25$ GeV. The light red bands on the left are excluded by chargino searches at LEP. In the gray wedge in the left-hand corner electroweak symmetry breaking conditions are not satisfied. The dark red region denoted 'χ NOT LSP' corresponds to the LSP being the lighter stau lepton. The large light orange regions of $\Omega_\chi h^2 > 0.3$ are excluded by cosmology while the narrow green bands correspond to the expected range $0.1 < \Omega_\chi h^2 < 0.2$. Also shown are the semi-oval contours of $a_\mu^{SUSY} = \Delta a_\mu^{SUSY}/10^{-10}$ favored by the anomalous magnetic moment of the muon measurement at 2σ ($a_\mu^{SUSY} = 11, 75$) and 1σ ($a_\mu^{SUSY} = 27, 59$). The 2σ range is shown in dark yellow. The three lines in the figure correspond respectively to $a_\mu^{SUSY} = 11, 27$ and 59, when moving towards the origin. The lines of the lightest Higgs scalar mass $m_h = 113$ GeV and 115 GeV are denoted by short and long-dash lines, respectively.

$11 < a_\mu^{SUSY}/10^{-10} < 75$

not robust

16

Roszkowski – Ruiz – T.N.
(JHEP 0108)

$\Omega h^2 < 0.3$
(cosmo. allowed)
thanks to A-pole!

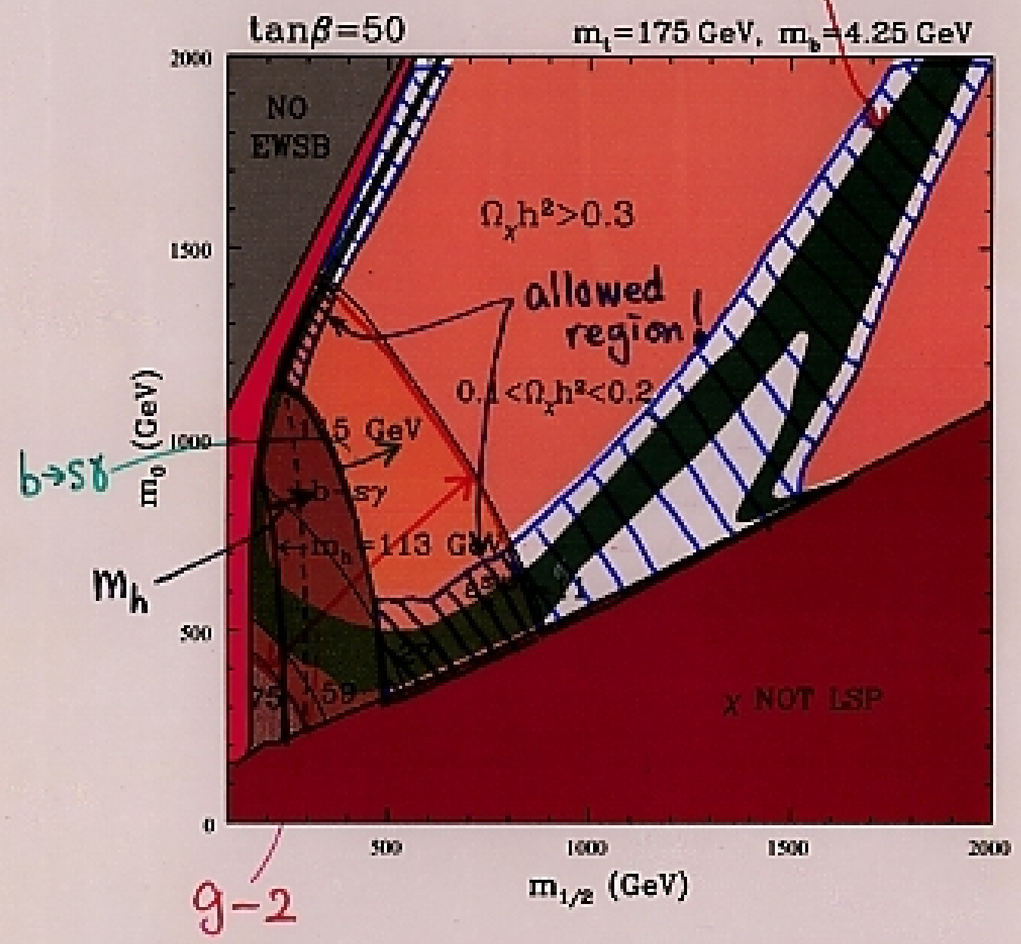

Figure 3: The same as in Fig. 2 but for $\tan\beta = 50$. The green band of the expected range $0.1 < \Omega_\chi h^2 < 0.2$ has now changed considerably due to the appearance of a wide resonance $\chi\chi \to A \to f\bar{f}$. The white areas closer (further away) from the axes correspond to $\Omega_\chi h^2 < 0.1$ ($0.2 < \Omega_\chi h^2 < 0.3$).

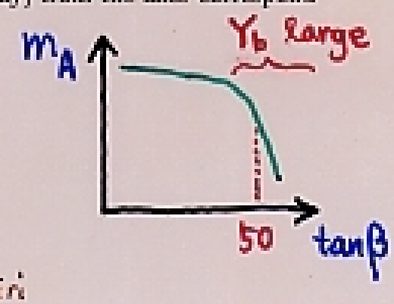

Allowed regions grow significantly as $\tan\beta \to 50$.
(A-pole effect)[18]
– Drees-Nojiri

Ellis - Olive - Santoso - Spanos
(PLB, 2003)

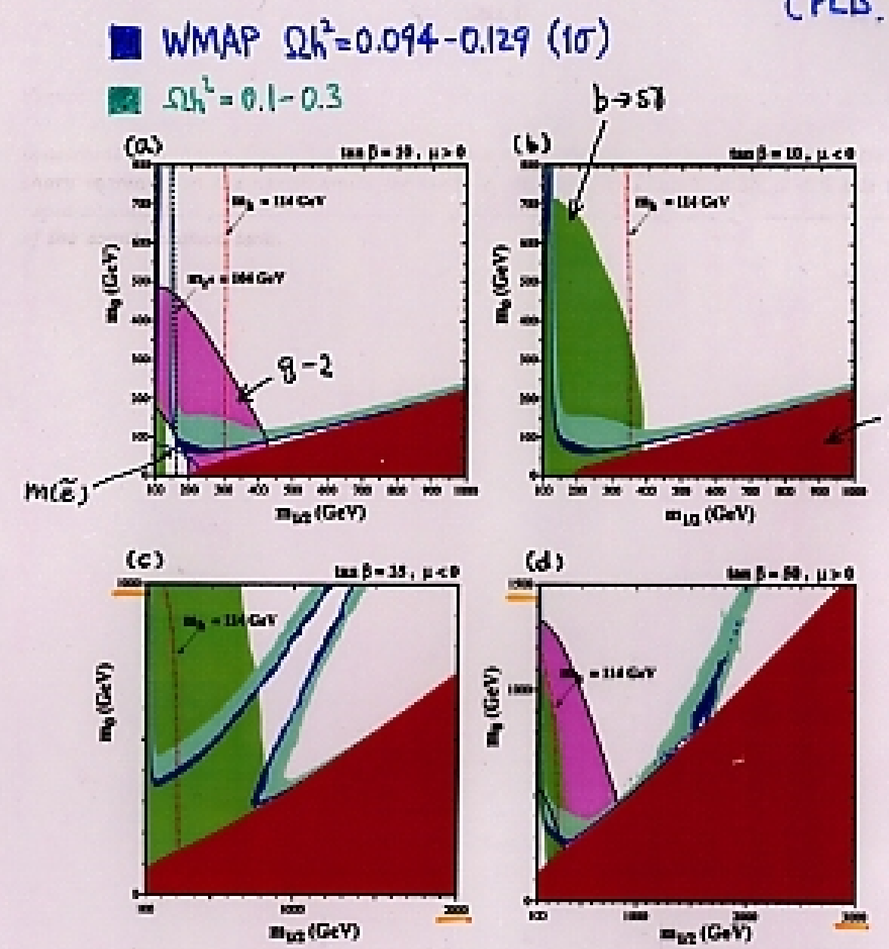

Figure 1: *The $(m_{1/2}, m_0)$ planes for (a) $\tan\beta = 10, \mu > 0$, (b) $\tan\beta = 10, \mu < 0$, (c) $\tan\beta = 35, \mu < 0$, and (d) $\tan\beta = 50, \mu > 0$. In each panel, the region allowed by the older cosmological constraint $0.1 \le \Omega_\chi h^2 \le 0.3$ has medium shading, and the region allowed by the newer cosmological constraint $0.094 \le \Omega_\chi h^2 \le 0.129$ has very dark shading. The disallowed region where $m_{\tilde{\tau}_1} < m_\chi$ has dark (red) shading. The regions excluded by $b \to s\gamma$ have medium (green) shading, and those in panels (a,d) that are favoured by $g_\mu - 2$ at the 8-σ level have medium (pink) shading. A dot-dashed line in panel (a) delineates the LEP constraint on the $\tilde{e}$ mass and the contours $m_{h^0} = 104$ GeV ($m_h = 114$ GeV) are shown as near-vertical black dashed (red dot-dashed) lines in panel (a) (each panel).*

Allowed "line"

Ellis-Olive-Santoso-Spanos
(2003)

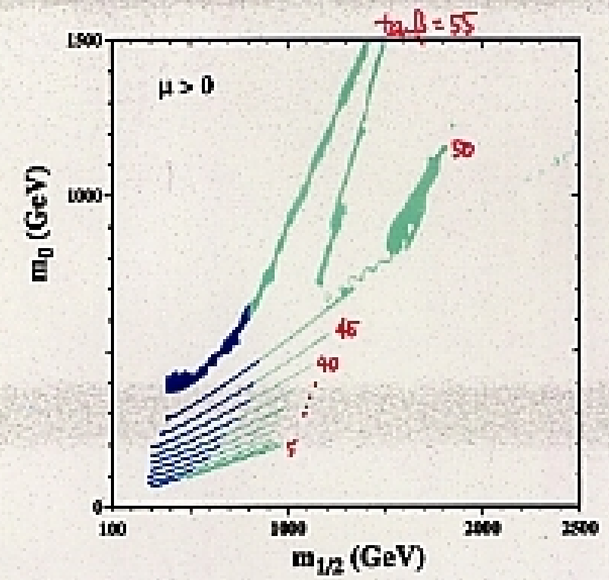

■ g−2 imposed

WMAP

Figure 2: *The strips display the regions of the $(m_{1/2}, m_0)$ plane that are compatible with $0.094 < \Omega_\chi h^2 < 0.129$ and the laboratory constraints for $\mu > 0$ and $\tan\beta = 5, 10, 15, 20, 25, 30, 35, 40, 45, 50, 55$. The parts of the strips compatible with $g_\mu - 2$ at the 2-σ level have darker shading.*

are considerably narrower than the spacing between them, though any intermediate point in the $(m_{1/2}, m_0)$ plane would be compatible with some intermediate value of $\tan\beta$. The right (left) ends of the strips correspond to the maximal (minimal) allowed values of $m_{1/2}$ and hence m_χ[3]. The lower bounds on $m_{1/2}$ are due to the Higgs mass constraint for $\tan\beta \leq 23$, but are determined by the $b \to s\gamma$ constraint for higher values of $\tan\beta$. The upper bound on $m_{1/2}$ for $\tan\beta \gtrsim 50$ is clearly weaker, because of the rapid-annihilation regions.

Also shown in Fig. 2 in darker shading are the restricted parts of the strips that are compatible with the BNL measurement of $g_\mu - 2$ at the 2-σ level, if low-energy e^+e^- data are used to calculate the Standard Model contribution [17]. If this constraint is imposed, the range of $m_{1/2}$ is much reduced for any fixed value of $\tan\beta$, and in particular the upper bound on $m_{1/2}$ is significantly reduced, particularly for $\tan\beta \gtrsim 50$. However, there is in

[3]The droplets in the upper right of the figure are due to coannihilations when $\tilde{\tau}$ is sitting on the Higgs pole. Here this occurs at $\tan\beta = 45$.

Ellis-Olive-Santoso-Spanos
(2003)

$\Omega_\chi h^2 < 0.129$

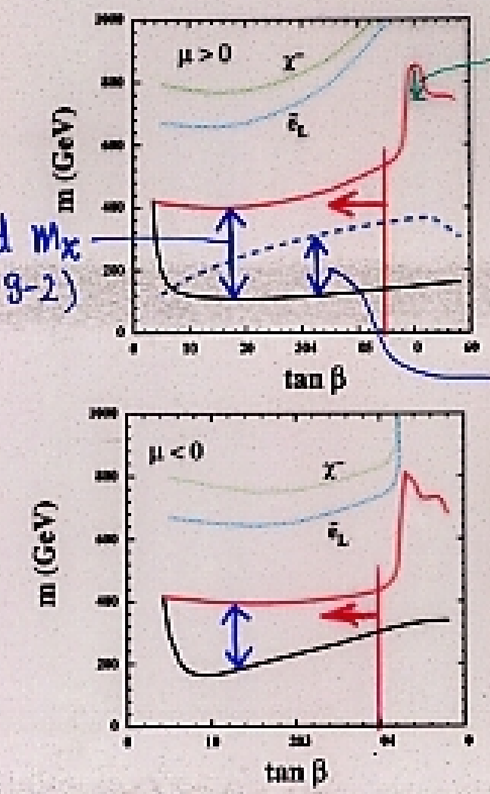

if $0.094 < \Omega_\chi h^2$

allowed m_χ (without g−2)

allowed m_χ (with g−2)

$m_\chi \lesssim 500$ GeV for $\tan\beta \lesssim 45$, $\mu > 0$ or $\tan\beta \lesssim 30$, $\mu < 0$

Figure 3: *The ranges of m_χ allowed by cosmology and other constraints, for (a) $\mu > 0$ and (b) $\mu < 0$. Upper limits without (red solid line) and with (blue dashed line) the $g_\mu - 2$ constraint are shown for $\mu > 0$: the lower limits are shown as black solid lines. Note the sharp increases in the upper limits for $\tan\beta \gtrsim 50, \mu > 0$ and $\tan\beta \gtrsim 35, \mu < 0$ due to the rapid-annihilation funnels. Also shown as dotted lines are the $\tilde{e}_L$ and $\chi^\pm$ masses at the tips of the coannihilation tails.*

$m_\chi \lesssim 700$ GeV for $0.1 < \Omega h^2 < 0.3$

V. Summary

■ CDM relic density from WMAP

$$\Omega_\chi h^2 = 0.1126^{+0.016}_{-0.018}$$

(χ : cold dark matter)

■ CMSSM

Constrained MSSM (CMSSM) is strongly constrained by WMAP.

- Allowed "line" in the $(m_0, m_{1/2})$ plane
- LSP mass upper bound: significantly reduced

$$m_\chi \lesssim 500\,\mathrm{GeV}$$

for $\tan\beta \lesssim 45$ and $\mu > 0$

or $\tan\beta \lesssim 30$ and $\mu < 0$

$\longrightarrow$ Increasing likelihood of finding superparticles at LHC , LC